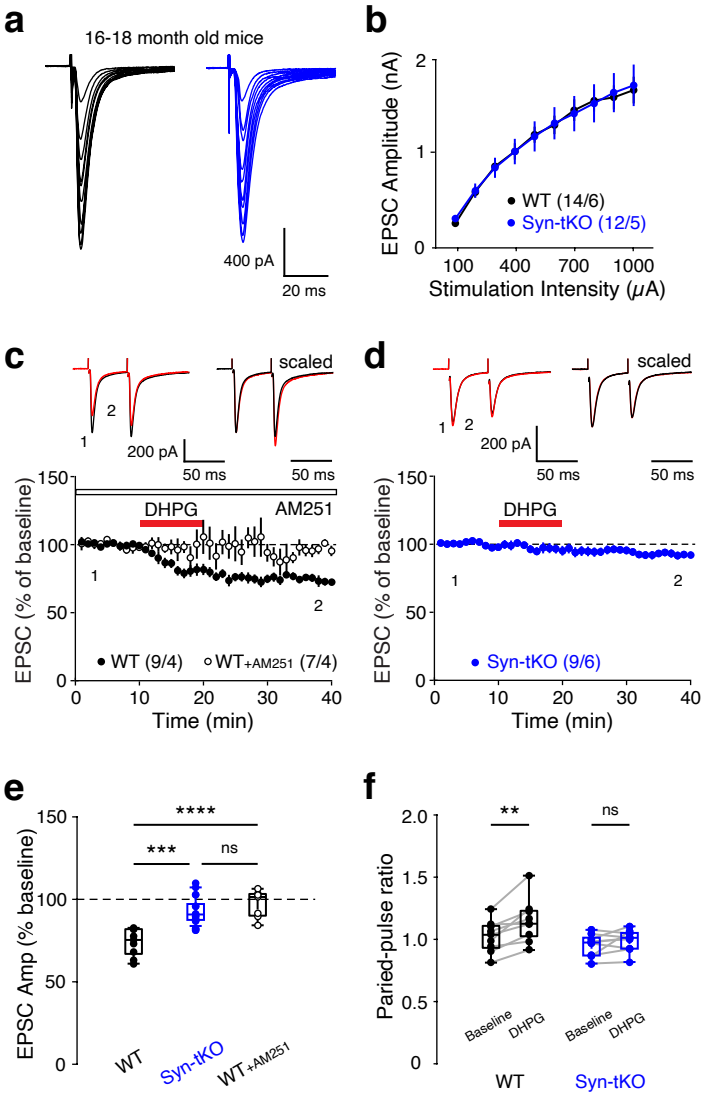

Albarran et al.,- Extended Data Figure 1

Extended Data Figure 1 | Normal corticostriatal input-output curves but impaired eCB-LTD in aged Syn-tKO mice. (**a**), Representative traces of evoked corticostriatal EPSCs in WT and Syn-tKO SPNs from aged mice (16-18 months old) across a range of stimulation intensities. (**b**), Normal input-output curves in Syn-tKO mice (WT: n = 14 cells / 6 mice; Syn-tKO: n = 12 cells / 5 mice; p = 0.960). (**c-e**), Summary of DHPG-mediated eCB-LTD in aged (16-18 months old) WT mice (**c**), which is fully blocked by the CB1R antagonist AM251 (10 μM) (WT: n = 9 cells / 4 mice, 73.88 ± 2.74%; WT + AM251: n = 7 cells / 4 mice, 97.06 ± 3.20%; p = 3.026e-5); top, representative traces. (**d**) eCB-LTD is impaired in aged Syn-tKO mice compared to WT (Syn-tKO: n = 9 cells / 6 mice, 92.57 ± 2.57%; p = 1.955e-4); top, representative trace. (**f**), Significant increase in aged WT PPRs (baseline: 1.02 ± 0.04; post-DHPG: 1.15 ± 0.06; p = 3.9e-3) but not in aged Syn-tKO PPRs (baseline: 0.95 ± 0.03; post-DHPG: 0.99 ± 0.03; p = 0.301). Data are mean ± s.e.m. Statistical significance was assessed by 2-way repeated measures ANOVA (**b**), ANOVA with multiple comparisons (**e**), and Wilcoxon signed tests (**f**) (**** p < 0.0001; *** p < 0.001; ** p < 0.01; n.s. non-significant).

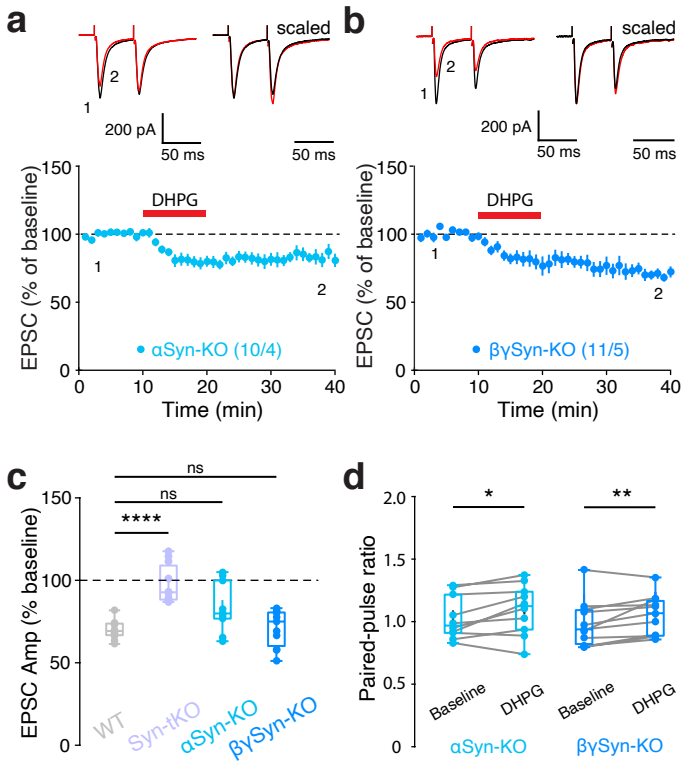

Albarran et al.,- Extended Data Figure 2

Extended Data Figure 2 | Normal DHPG-LTD in α-Syn-KO and βγ-Syn-KO mice. (**a-c**), DHPG-mediated eCB-LTD is normal in (**a**) α-Syn-KO (WT data from Fig. 1: n = 11 cells / 4 mice, 69.95 ± 1.70%; α-Syn-KO: n = 10 cells / 4 mice, 83.44 ± 4.67%; p = 0.162) and (**b**) βγ-Syn-KO mice (n = 11 cells / 5 mice, 71.00 ± 3.38%; p = 0.957). (**d**), Significant increases in PPR in both α-Syn-KO (baseline: 1.03 ± 0.05; post-DHPG: 1.10 ± 0.06; p = 0.037) and βγ-Syn-KO mice (baseline: 0.98 ± 0.06; post-DHPG: 1.05 ± 0.05; p = 9.8e-3). Data are mean ± s.e.m. Statistical significance was assessed by ANOVA with multiple comparisons (**c**), and Wilcoxon signed tests (**d**) (**** $p < 0.0001$; ** $p < 0.01$; * $p < 0.05$; n.s. non-significant).

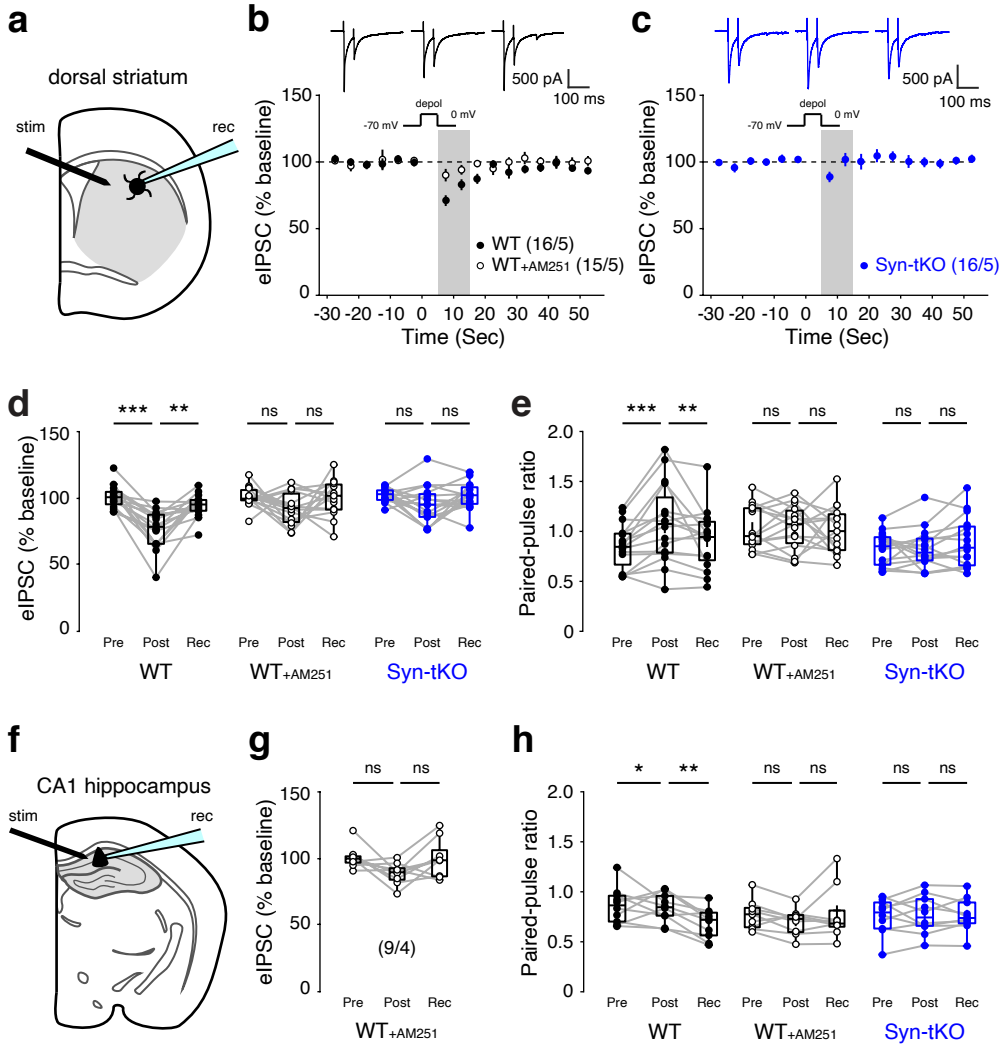

Albarran et al.,- Extended Data Figure 3

Extended Data Figure 3 | DSI is impaired in the dorsal striatum and CA1 of hippocampus of Syn-tKO mice. (**a**), Schematic of evoked DSI experiments in the dorsal striatum. (**b-d**), Summary of DSI (evoked IPSCs) in recorded SPNs in the dorsal striatum of WT mice (n = 16 cells / 5 mice; pre-depol: 100.94 ± 2.09%; post-depol: 76.95 ± 3.64%; recovery: 94.43 ± 2.16%; p = 4.378e-4, p = 7.764e-4), which is blocked by AM251 (10 µM) (n = 15 cells / 5 mice; pre-depol: 101.15 ± 1.99%; post-depol: 92.13 ± 3.14%; recovery: 99.97 ± 3.50%; p = 0.055, p = 0.277). Striatal DSI is impaired in Syn-tKO mice (**c, d**) (n = 16 cells / 5 mice; pre-depol: 102.19 ± 1.29%; post-depol: 95.25 ± 3.54%; recovery: 101.64 ± 2.53%; p = 0.134, p = 0.134). (**e**), Significant transient increases in PPR during striatal DSI in WT cells (pre-depol: 0.85 ± 0.06; post-depol: 1.08 ± 0.10; recovery: 0.92 ± 0.07; p = 2.3e-3, p = 0.030) but not in WT cells in the presence of AM251 (pre-depol: 1.04 ± 0.06; post-depol: 1.04 ± 0.06; recovery: 1.01 ± 0.06; p = 0.847, p = 0.600) or in Syn-tKO cells (pre-depol: 0.83 ± 0.04; post-depol: 0.82 ± 0.05; recovery: 0.89 ± 0.06; p = 0.959, p = 0.134). (**f**), Schematic of evoked DSI experiments in CA1 of the hippocampus. (**g**), Summary of DSI in recorded principal neurons in CA1 of WT mice in the presence of AM251 (10 µM) (n = 9 cells / 4 mice; pre-depol: 101.17 ± 2.82%; post-depol: 89.22 ± 2.67%; recovery: 100.26 ± 4.74%; p = 0.055, p = 0.098). (**h**), Significant transient increases in PPR during hippocampal DSI in WT cells (pre-depol: 0.69 ± 0.06; post-depol: 0.84 ± 0.05; recovery: 0.69 ± 0.05; p = 0.037, p = 5.9e-3) but not in WT cells in the presence of AM251 (pre-depol: 0.77 ± 0.05; post-depol: 0.70 ± 0.04; recovery: 0.78 ± 0.09; p = 0.098, p = 0.570) or in Syn-tKO cells (pre-depol: 0.75 ± 0.06; post-depol: 0.77 ± 0.06; recovery: 0.77 ± 0.05; p = 0.770, p = 1.000). Data are mean ± s.e.m. Statistical significance was assessed by Wilcoxon signed tests (**d, e, g, h**) (*** p < 0.001; ** p < 0.01; * p < 0.05; n.s. non-significant).

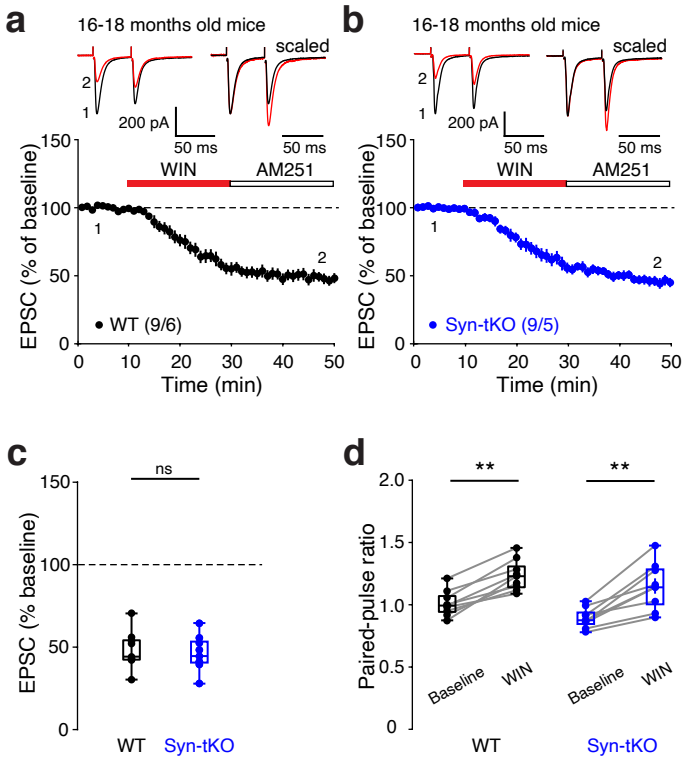

Albarran et al.,- Extended Data Figure 4

Extended Data Figure 4 | Normal WIN-LTD in aged Syn-tKO mice. (**a-c**), WIN application results in indistinguishable corticostriatal LTD in aged (16-18 months) WT and aged Syn-tKO mice (WT: n = 9 cells / 6 mice, 48.11 ± 3.78%; Syn-tKO: n = 9 cells / 5 mice, 46.01 ± 3.56%; p = 0.605). (**d**), Significant increases in PPRs in both aged WT (baseline: 1.02 ± 0.03; post-WIN: 1.24 ± 0.04; p = 3.9e-3) and aged Syn-tKO mice (baseline: 0.90 ± 0.03; post-WIN: 1.16 ± 0.06; p = 3.9e-3). Data are mean ± s.e.m. Statistical significance was assessed by Mann-Whitney (**c**) and Wilcoxon signed tests (**d**) (** p < 0.01; n.s. non-significant).

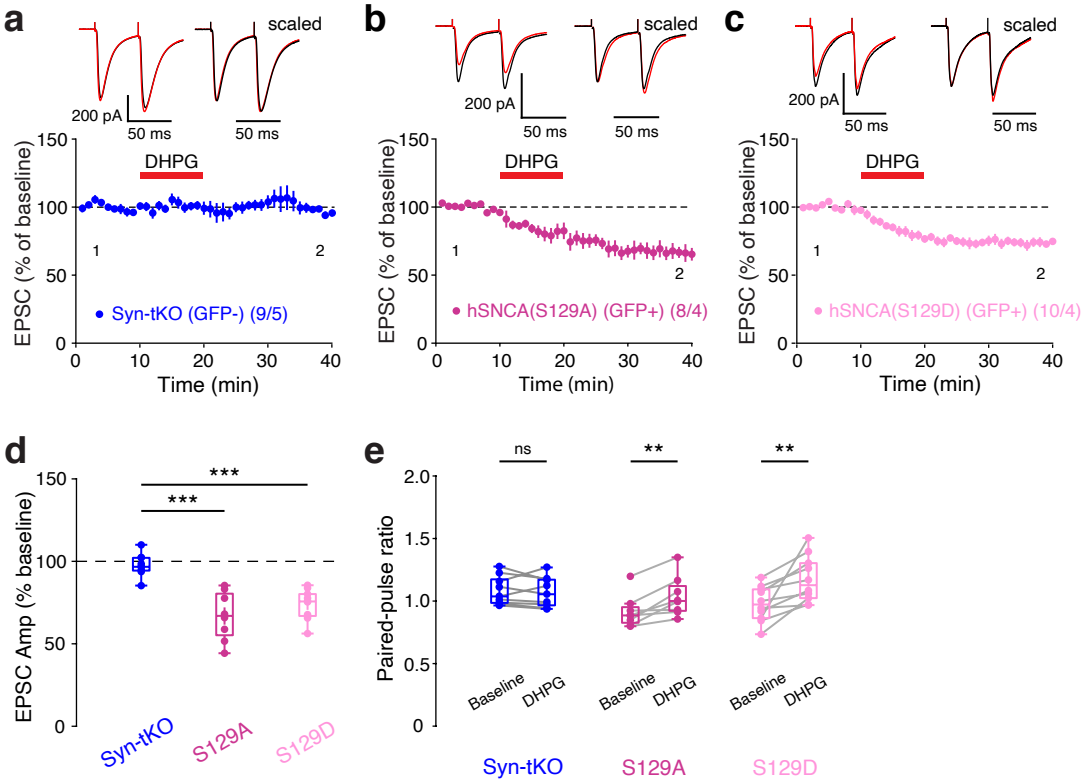

Albarran et al.,- Extended Data Figure 5

Extended Data Figure 5 | α-Syn S129A (phospho-deficient) and α-Syn S129D (phosphor-mimic) mutations do not disrupt viral α-Syn rescue of eCB-LTD. (**a-d**), Neither S129A (b) nor S129D (**c**) mutations affected the ability of postsynaptic viral α-Syn to rescue eCB-LTD (GFP-, pooled: n = 9 cells / 5 mice, 97.54 ± 2.28%; GFP+, S129A: n = 8 cells / 4 mice, 66.89 ± 5.24%; p = 1.03e-5; GFP+, S129D: n = 10 cells / 4 mice, 73.62 ± 2.89%, p = 1.39e-4). (**e**), Significant PPRs observed in cells infected with S129A α-Syn (baseline: 0.91 ± 0.05; post-DHPG: 1.04 ± 0.06; p = 7.8e-3) and S129D α-Syn (baseline: 0.98 ± 0.04; post-DHPG: 1.18 ± 0.06; p = 2.0e-3), but not in uninfected cells (baseline: 1.08 ± 0.04; post-DHPG: 1.07 ± 0.04; p = 0.496). Data are mean ± s.e.m. Statistical significance was assessed by ANOVA with multiple comparisons (**d**) and Wilcoxon signed tests (**e**) (*** $p < 0.001$; ** $p < 0.01$; n.s. non-significant).

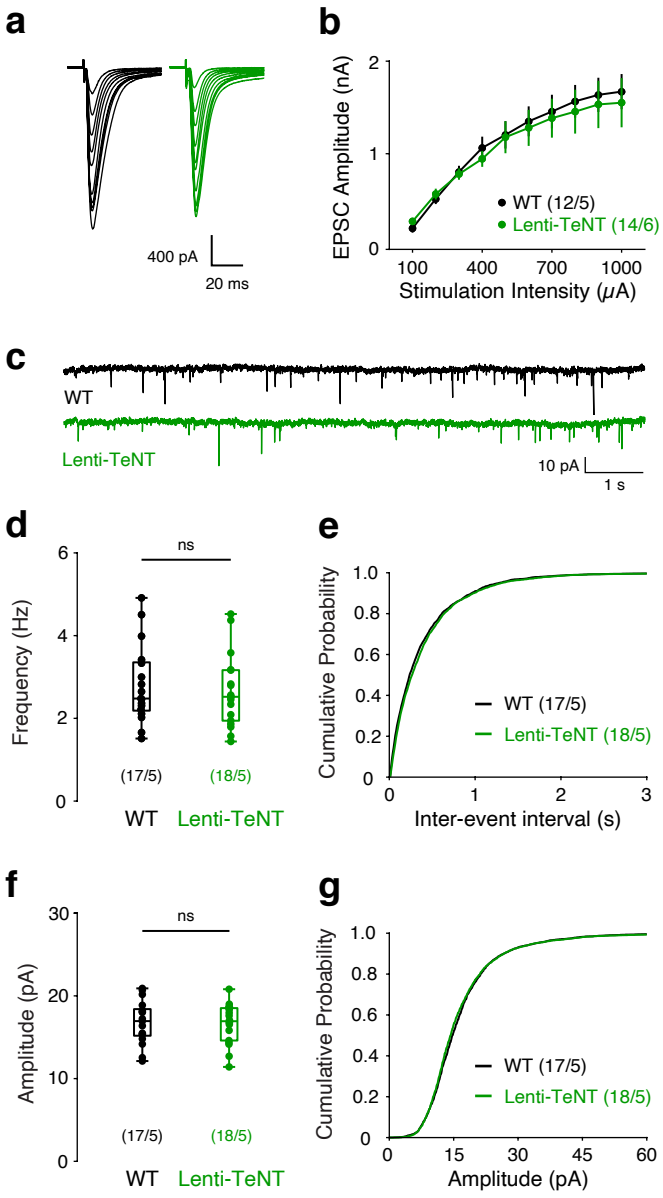

Albarran et al.,- Extended Data Figure 6

Extended Data Figure 6 | Lentiviral TeNT does not disrupt basal synaptic properties of striatal SPNs. (**a**), Representative traces of evoked corticostriatal EPSCs in WT (GFP-) and TeNT-infected (GFP+) SPNs across a range of stimulation intensities. (**b**), Normal input-output curves in TeNT-expressing SPNs (GFP-: n = 12 cells / 5 mice; GFP+: n = 14 cells / 6 mice; p = 0.787). (**c**), Representative traces of mEPSC recordings from WT (GFP-) and TeNT-expressing (GFP+) cells. (**d-g**), Lentiviral TeNT does not result in a change in (**d, e**) mEPSC frequency (GFP-: n = 17 cells / 5 mice, 2.81 ± 0.22 Hz; GFP+: n = 18 cells / 5 mice, 2.64 ± 0.20 Hz; p = 0.680) or in (**f, g**) mEPSC amplitude (GFP-: 16.78 ± 0.62 pA; GFP+: 16.65 ± 0.55 pA; p = 0.987). Data re mean ± s.e.m. Statistical significance was assessed by 2-way repeated measures ANOVA (**b**) and Mann-Whitney tests (**d, f**) (n.s. non-significant).